World Applied Sciences Journal 13 (12): 2536-2544, 2011
ISSN 1818-4952

A Novel Passive Filter to Reduce PWM Inverters Adverse Effects in Electrical Machine System

[1]*Abdolreza Esmaeli and* [2]*Fazel Tavassoli*

[1]Reactors and Accelerators Research and Development School,
Nuclear Science and Technology Research Institute, P.O. Box 14155-1339, Tehran, Iran
[2]Department of Electrical Engineering, Maziar University, Nour, Royan, P.O. Box: 511

Abstract: A novel passive filter to reduce PWM inverter's adverse effects in electrical machine system is studied in this paper. A PWM inverter fed ac induction motor drive system capable of suppressing all the adverse effects of PWM inverter to provide a robust control system is developed. A passive electromagnetic interference (EMI) filter developed for this system is characterized by sophisticated connection of two small passive filters between inverter output and motor which can compensate for common mode voltages produced by PWM inverter and between motor neutral point and rectifier input capable of suppressing leakage current. As a result small passive filter capable of reducing all the adverse effects is approached. The reduction characteristics of the shaft voltage, bearing current, common mode current, leakage current and EMI are approached by modeling, simulation and experimental results.

Key words: EMI filter . EMC . electrical machine . PWM inverter

INTRODUCTION

Electromagnetic compatibility of power electronic systems becomes an engineering discipline and it should be considered at the beginning stage of a design. Thus, a power electronics design becomes more complex and challenging and it requires a good communication between EMI and Power electronics experts. The rise of switching frequency combined with micro-electronic improvements enable to reduce active components sizes and so convertors sizes. This rise has also made EMC problems worse and now, filters have to be more and more effective on larger frequency range. Nowadays, conducted electromagnetic emissions produced by adjustable-speed AC drive systems become the main interested subject for researchers and industry Modern pulse width modulation (PWM) inverters are widely used in industrial, commercial and residential application such as motor drives [1, 2].

In three-leg inverters for three-phase applications the occurrence of common mode voltage is inherent due to asymmetrical output pulses. It has been found that the high dv/dt and high switching frequency together with the common mode voltages generated by PWM inverters have caused many adverse effects such as shaft voltage, bearing current, leakage current and electromagnetic interference (EMI). The EMI generated by such systems is increasingly causing concerns, as the EMC regulations become more stringent. In order to comply with these international EMC regulations, an EMI filter is often necessary.

The current researchers up till now have only provided solutions for one or two isolated side effects and no collective solutions have yet been proposed. Some of them concerning passive and active EMI filters have focused on eliminating high frequency leakage current [3, 4] shaft voltage and bearing current [5-8] and EMI [9-14].

The major objective of this research is to investigate and suppress of the adverse effects of PWM inverter in electrical machine system. This paper discusses a passive cancellation method for the purpose of elimination the adverse effects of PWM inverter based on modeling, simulation and experimental results. The simulation platform SABER is chosen because of the robust modeling engine, the ease of integrating mechanical components and the large library of existing models for a wide range of electrical components. SABER provides a good platform for device performance prediction in a system environment and also reliable data for EMI noise determinations [15]. This paper includes seven parts. First part gives introduction. Second part gives high frequency models of rectifier, dc link, inverter and induction. Third part gives system analysis as different mode and common mode EMI and proposed filter analysis. Part 4 gives simulated results based on the presented models and the parameters of the induction motor systems. The 6 kVA

Corresponding Author: Mr. Fazel Tavassoli, Department of Electrical Engineering, Maziar, Nour, Iran, P.O. Box. 511

inverter by 10 kHz switching frequency fed three-phase 3.7 kW (1750 rpm) induction motor in this paper. Part 5 gives the experimental results and finally the conclusion and references are given in part 6 and 7 respectively.

MODELING

For an accurate High Frequency (HF) model of AC motor drive systems, the HF parasitic current paths should take into account [16, 17]. Fig. 1 shows the PWM inverter fed ac motor drive system configuration without EMI filter. Also coupling routes of conducted EMI noise are shown in this figure.

Rectifier and DC link: The HF equivalent circuit of rectifier and DC link is shown in Fig. 2. As an important role of parasitic capacitances between anode of diodes and ground in the HF current paths is considered in HF model of three-phase rectifier, C_{P1} is the parasitic capacitance of upper and C_{P2} is the parasitic capacitance of lower diodes in the rectifier shown in Fig. 2. R_p and L_p are resistance and inductance parasitic value of DC capacitor of DC link.

Inverter: The three-phase inverter consisting of six IGBTs and six soft recovery diodes is used to drive the motor. The equivalent circuit of the three-phase voltage source inverter (VSI) is obtained by an extension of the switching cell.

The inverter is composed of three legs, each of which consisting of two power IGBTs with parallel freewheeling diodes. The HF circuit model of the inverter system must take the main parasitic components of the inverter into account. Stray inductances of the connecting wires and parasitic capacitances between IGBT and heatsink are considered in the model. HF equivalent circuit of one leg of three-phase IGBT inverter is shown in Fig. 3.

L_L is stray inductance of the connecting wires. C_P is stray capacitance of the collector and grounded heatsink. Between the collector and the heatsink, there appears a stray capacitance that affects principally leakage current generation.

L_E and L_C are parasitic inductances of the emitter and collector of IGBT Model. Differential conducted emissions are affected by these inductances.

L_a is the a-phase line parasitic inductance and L_{L1} to L_{L4} are the line parasitic inductances from base and collector to PWM sources. Also the heatsink is modelled by one inductor (L_H) and one resistor (R_H).

The value of the parasitic elements approached from measurements and devices datasheets for rectifier, DC link and inverter are presented in Table 1. All impedance measurements were performed with a resistance, inductance and capacitance (RLC) meter with a measurement range of 75 kHz–30 MHz, following a proper calibration via a short-open procedure [18].

Induction motor: A novel induction motor's model is shown in Fig. 4. R, L and C are distributing parameters representing the HF coupling between the stator windings and rotor assembly. Because of the partial insulation effect of the bearing grease and the EDM effect between the bearing balls and races, the motor bearings can be modeled as a capacitance C_b in parallel to a non-linear resistive circuit (R_L) and series with bearing ball and race contact resistance R_b. The bearing

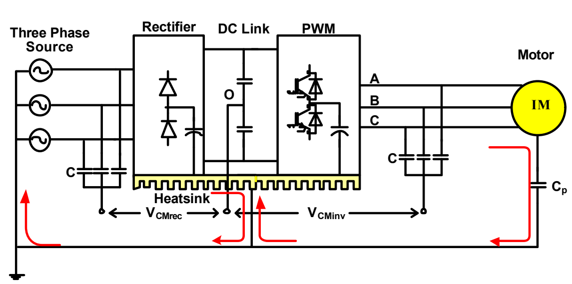

Fig. 1: PWM inverter fed ac motor drive system configuration whithout EMI filter

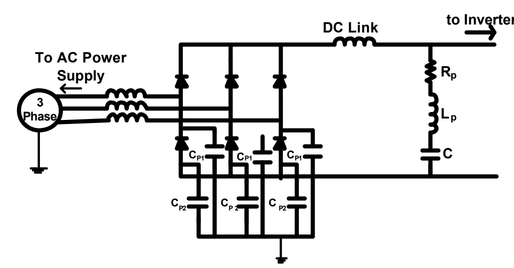

Fig. 2: HF equivalent circuit of rectifier and DC link

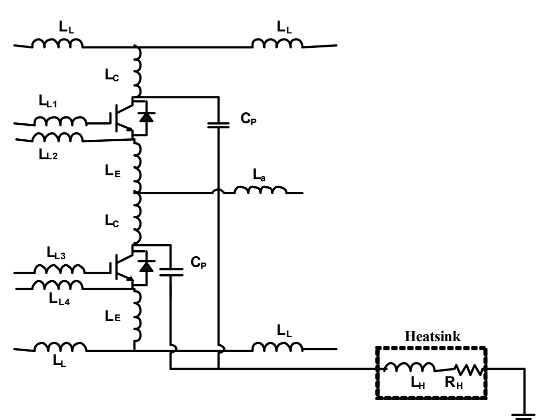

Fig. 3: HF equivalent circuit of one leg of three-phase inverter

Table 1: The HF Parameters value of rectifier, DC link and inverter

C_{p1}	C_{p2}	R_p	L_p	C	L_L, L_E, L_C
74 pF	29 pF	2 O	25 nH	2.2 mF	3 nH
L_1, L_3	L_2, L_4	L_a	L_H	R_H	C_P
30 nH	50 nH	15 nH	125μH	8 O	220 pF

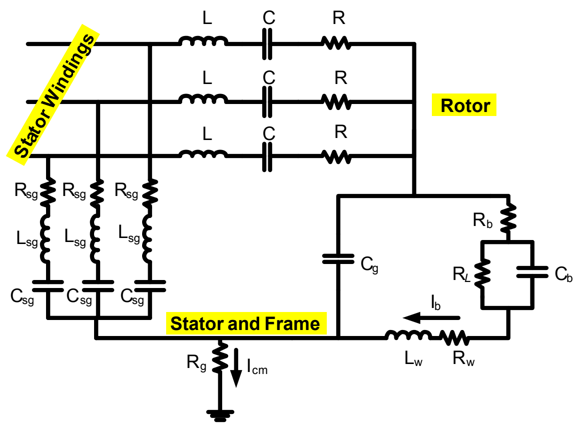

Fig. 4: The HF model of induction motor

current, I_b, is flowing through the modeled wire impedance of measuring bearing current (L_w and R_w). C_g is the capacitance present across the stator and the motor laminations across the motor air gap.

The coupling between the stator windings and the frame (stator) is considered as inductance (L_{sg}), resistance (R_{sg}) and capacitance (C_{sg}) since it mainly contributes the total leakage current into the ground. Frame is modeled as resistance of R_g to ground.

The values of HF parameters model of induction motor are presented in Table 2.

By considering Fig.1, the common mode voltage can be calculated by the following equation:

$$V_{CM} = \frac{V_{AG} + V_{BG} + V_{CG}}{3} = \frac{V_{AO} + V_{BO} + V_{CO}}{3} + V_{OG} = V'_{CM} + V_{OG} \quad (1)$$

where V_{AG}, V_{BG}, V_{CG}, V_{OG} represent the electric potential of point A, B, C, respectively, V_{AO}, V_{BO}, V_{CO} represent the voltage across A, B, C and O respectively.

To simplify the equation 1 can be written as (2) using switching function S_i (i=A, B, C), S_i=1 representing bottom switch being on.

$$V_{CM} = \frac{(S_A + S_B + S_C)U_d}{6} + V_{OG} = \begin{cases} \pm\frac{U_d}{2} + V_{OG} \\ \pm\frac{U_d}{6} + V_{OG} \end{cases} \quad (2)$$

where V_{OG} is the electric potential of point O.

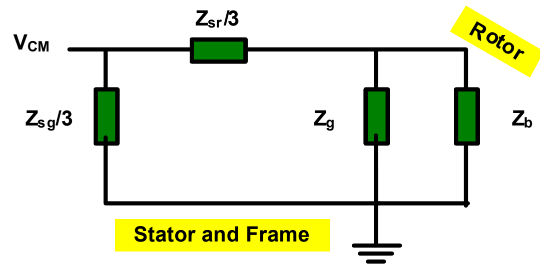

Fig. 5: Simplified model of induction motor

By considering the simplified model of induction motor shown in Fig. 5 shaft voltage can be calculated by (3).

$$V_{sh} = V_{CM} \times \frac{Z_{rg}}{\frac{Z_{sr}}{3} + Z_{rg}} \quad (3)$$

where Z_{sr} is the impedance between the stator windings and rotor and impedance between the rotor and frame is Z_{rg} as defined in the following:

$$Z_{rg} = \frac{Z_g \times Z_b}{Z_g + Z_b}, Z_{sr} = R + JL\omega + \frac{1}{JC\omega} \quad (4)$$

where Z_b and Z_g calculated as

$$Z_b = \frac{R_L \times \frac{1}{JC_b\omega}}{R_L + \frac{1}{JC_b\omega}} + R_b + R_W + JL_W\omega \quad (5)$$

$$Z_g = \frac{1}{JC_g\omega} \quad (6)$$

So the bearing current can be calculated by (7).

$$I_b = \frac{V_{sh}}{Z_b} \quad (7)$$

and leakage current can be developed as:

$$I_c = \frac{V_{CM}}{Z_{sg}/3} + \frac{V_{sh}}{Z_g} + \frac{V_{sh}}{Z_b} \quad (8)$$

where Z_{sg} is the impedance between the stator winding and ground.

Table 2: The HF parameters value of induction motor

R_w	L_w	L	C	R	C_g
9 O	0.5µH	275 µH	19 pF	178 O	820 pF
R_L	R_b	C_b	R_{sg}	L_{sg}	C_{sg}
89 kO	3 O	180pF	138 O	14 µH	800pF

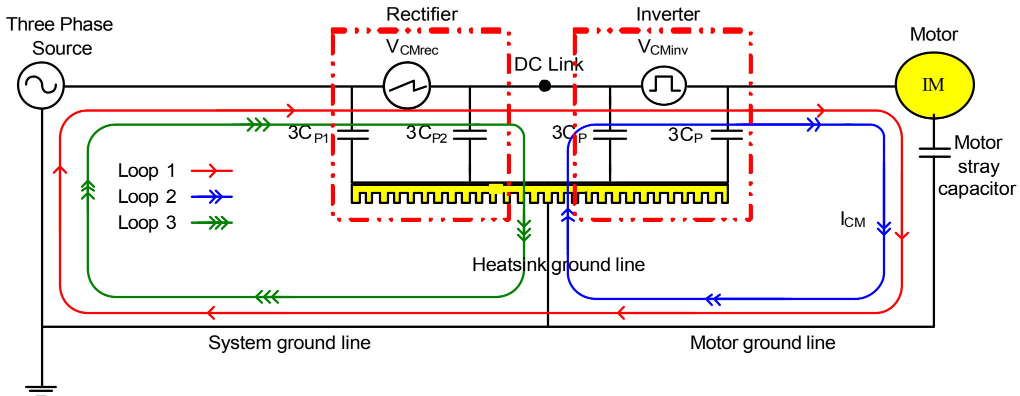

Fig. 6: Common mode equivalent circuit of PWM inverter fed ac motor drive system of Fig. 1

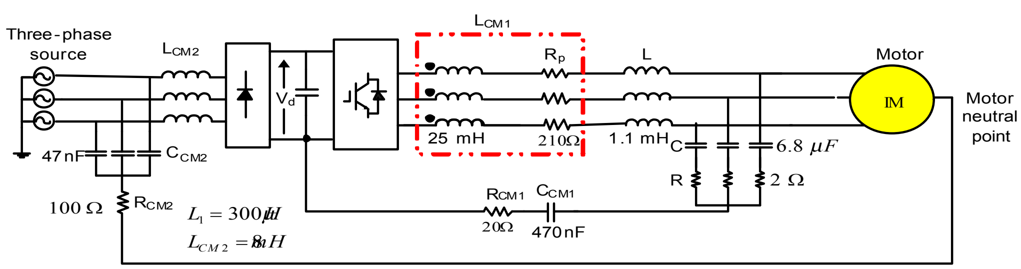

Fig. 7: The system configuration when the proposed passive filter is connected

$$Z_{sg} = R_{sg} + JL_{sg}\omega + \frac{1}{JC_{sg}\omega} \qquad (9)$$

SYSTEM ANALYSIS

In Fig. 1 three possible loops of common mode current in PWM inverter fed ac motor drive system (Fig. 1) are illustrated by an equivalent circuit shown in Fig. 6. These three current loops are:

Loop 1: Inverter → motor stray capacitor → motor ground line → system ground line → mains → rectifier → inverter

Loop 2: Inverter → motor stray capacitor → motor ground line → heat sink ground line → heat sink → device parasitic capacitors → inverter

Loop 3: Inverter → device parasitic capacitors → heat sink → heat sink ground line → system ground line → mains → rectifier → inverter

Generally, a three-phase diode module and a three-phase insulated gate bipolar transistors (IGBT) module are attached on a common heat sink. This means that the common mode voltage produced by the rectifier, V_{CMrec} and that by the inverter, V_{CMinv}, cause common mode voltages to the ungrounded heat sink because non-negligible parasitic capacitors exist inside the two electrically insulated diode and IGBT modules in Fig. 1. Fig. 7 shows the circuit configuration of PWM inverter fed ac motor drive system connecting a small passive EMI filter at the output of a voltage-source PWM inverter and at input of rectifier. The inverter has a digital PWM controller in which three-phase sinusoidal balanced reference signals are compared with a repetitive triangular carrier signal with a

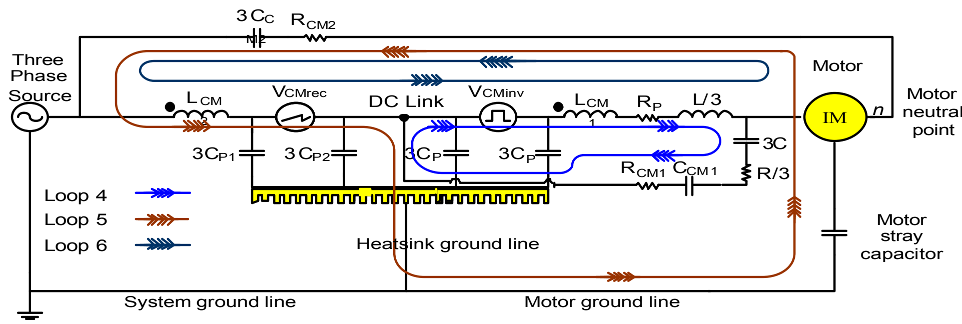

Fig. 8: Common mode equivalent circuit (Loops 1 to 3 have similar direction as Fig. 6)

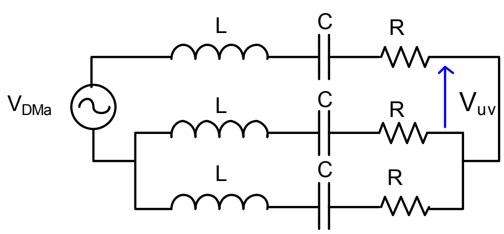

Fig. 9: Differential mode equivalent circuit

frequency of 10 kHz in order to generate the gate signals for the IGBTs. This filter requires access to ungrounded motor neutral point. It consists of three differential mode inductors, a common mode choke in inverter output and another common mode choke in rectifier input, six capacitors and four resistors. A set of three inductors L, three capacitors C and three resistors R forms a differential mode filter that eliminates high-frequency differential mode voltages from three-phase line-to-line voltages. It can damp out the over voltage appearing at the motor terminals. Although its installation makes the line-to-line voltages sinusoidal, it produces no effect on each line-to-neutral voltage.

The common mode filter consists of two common mode chokes L_{CM1}, C_{CM1}, R_{CM1} and L_{CM2}, three Y-connected capacitors, C_{CM2} and a damping resistor R_{CM2} that is connected between the motor neutral point and the capacitor neutral point.

Common mode and differential mode equivalent circuit model of the filter is presented in Fig. 8 and Fig. 9 respectively.

Design of differential mode filter: Fig. 9 shows the differential mode equivalent circuit where the motor inductance parameters are disregarded from high-frequency differential mode voltage and current points of view. This means that the inductance and capacitance values in the differential mode circuit are 3L/2 and 2C/3, respectively. Because a relation of $3\omega L/2=3/(2\omega C)$ exists at the carrier frequency of 10 kHz, it is not the capacitor but the inductor that determines the amplitude of the current. Note that the common mode choke is eliminated from Fig. 9 because it makes no contribution to the differential mode equivalent circuit.

The switching ripple current flowing through the inductor should be less than 10%, that is about 2 A in this case. When the differential mode voltage in Fig. 9 is assumed to be a sinusoidal waveform with amplitude of $V_d/2=269$ V and a carrier frequency of 10 kHz, the following is given the L value:

$$x_L \times i_r > \frac{V_d/2}{\sqrt{2}} \rightarrow \frac{3\times 2\pi \times 10000\times L}{2}\times 2 > \frac{269}{\sqrt{2}} \rightarrow L > 1\text{ mH} \qquad (10)$$

Hence, the inductance value was decided as 1.1 mH. The resonant frequency of the differential mode filter should be in the 1 kHz to 3 kHz range, taking into account both the maximum inverter output frequency of 50 Hz and the carrier frequency of 10 kHz. The resonant frequency was chosen to be 1.8 kHz so that the value of capacitor computes out to be 6.8 μF. The characteristic impedance given by $Z_o=(L/C)^{1/2}$ is nearly equal to 12O. The resistance value of R is considered 2O to the total loss dissipated in the three damping resistors be less than 0.1% of the rated inverter capacity (6 kVA).

Design of common mode filter: Fig. 8 shows a common mode equivalent circuit of the configuration system presented in Fig. 7. The equivalent circuit described in Fig. 8 makes clear the effect of the EMI filter on eliminating the common mode voltage from the motor terminals. This equivalent circuit helps to conclude that installation of the EMI filter yields the following current loops.

Loop 1: Inverter → common mode choke (L_{CM1}) → L/3 → motor stray capacitor → motor ground line →

system ground line $\rightarrow$ mains $\rightarrow$ common mode choke (L_{CM2}) $\rightarrow$ rectifier $\rightarrow$ inverter

Loop 2: Inverter $\rightarrow$ common mode choke (L_{CM1}) $\rightarrow$ L/3 $\rightarrow$ motor stray capacitor $\rightarrow$ motor ground line $\rightarrow$ heat sink ground line $\rightarrow$ heat sink $\rightarrow$ device parasitic capacitors $\rightarrow$ inverter

Loop 3: Inverter $\rightarrow$ device parasitic capacitors $\rightarrow$ heat sink $\rightarrow$ heat sink ground line $\rightarrow$ system ground line $\rightarrow$ mains $\rightarrow$ common mode choke (L_{CM2}) $\rightarrow$ rectifier $\rightarrow$ inverter

Loop 4: Inverter $\rightarrow$ common mode choke (L_{CM1}) $\rightarrow$ DM filter (L/3, 3C, R/3) $\rightarrow$ DC Link $\rightarrow$ inverter

Loop 5: Inverter $\rightarrow$ device parasitic capacitor $\rightarrow$ heat sink $\rightarrow$ heat sink ground line $\rightarrow$ motor ground line $\rightarrow$ motor neutral line (R_{CM2} and $3C_{CM2}$) $\rightarrow$ CM inductor (L_{CM2}) $\rightarrow$ inverter

Loop 6: Inverter $\rightarrow$ common mode choke (L_{CM1}) $\rightarrow$ L/3 $\rightarrow$ motor neutral line (R_{CM2} and $3C_{CM2}$) $\rightarrow$ CM inductor (L_{CM2}) $\rightarrow$ inverter

By evaluation of the considered loops of Fig. 8, it is obvious that the common mode choke, L_{CM1}, has no any effect in attenuating the common mode currents on loops 3 and 5. This shows that the circuit requires installing another small-sized common mode choke, L_{CM2}, at the rectifier input. The common mode voltage with dc and ac components is characterized by a step-changed voltage resulting from PWM operation as shown in Fig. 10. Note that the fundamental frequency of the ac components is equal to the carrier frequency of 10 kHz. The dc component is applied across the capacitor C_{CM1}, while the ac components are applied across the inductor L_{CM1}.

Since the flux produced in the inductor is given by the integration of the ac components with respect to time, it is reasonable to take into account the effect of the carrier-frequency component presented in the common mode voltage on flux saturation, neglecting other high-frequency components. The Faraday's law leads us to the following relation between the flux in the inductor and the common-mode voltage:

$$\phi = \frac{1}{N}\int V_{CM}dt \quad (11)$$

where N is the turn number per phase of the inductor, F is flux in the inductor and V_{CM} is common mode voltage. The flux density, B is given by

$$B = \frac{\phi}{S} = \frac{1}{SN}\int V_{CM}dt \quad (12)$$

where S is the cross section area of the core. For a given value of carrier frequency and a known value of common mode voltage, the product SN dictates the value of B_{max}. Alternatively, the product SN can be designed if the value of B_{max} is allowed not to exceed the saturation flux density B_{sat} of the core material used. A soft magnetic material having a crystalline structure in the nano-scale range is selected as the core material. This material has a saturation flux density as high as B_{sat}=1.2 T. Generally, the inductance value of an inductor without air gap is give by:

$$L_{CM} = \frac{\mu SN^2}{l} \quad (13)$$

where l is the mean core length and μ is the core permeability. A peak value of common mode current, I_{CMpeak} is inverse-proportional to the inductance value of LCM and therefore it is proportional to a value of l/N as long as SN is constant. The shorter the mean core length and the larger the number of turns, the smaller will be the peak value of the common mode current.

However, the number of turns cannot be increased beyond a certain limit because that would need a larger core and would result in a larger mean core length. This means that there exists an optimal value of l/N ratio, which is dependent on the diameter of the copper windings used, or in other words, on the current rating of the inductor. Based on the above discussions, the following common mode choke is designed and constructed: an inductor with a maximum flux density of 0.8 T at 40 Hz, which is 2/3 of the flux density of magnetic saturation. Note that a resonant frequency for the common mode circuit should be placed in a range of about 1.5 kHz, so that the capacitance value of CCM is designed as practical value of 470 nF by considering (14).

$$f = \frac{1}{2\pi\sqrt{L_{CM}C_{CM}}} \quad (14)$$

So L_{CM1} is found as 25mH with characteristic impedance of 210 O that is shown in Fig. 7 as R_p. The resistance value of R_{CM1} was designed as 20 O. Finally R_{CM2}, L_{CM2} and C_{CM2} considered as 100 O, 8 mH and 47 nF respectively.

SIMULATION RESULTS

The system without filter (Fig. 1) and with the proposed filter (Fig. 7) is simulated by Saber software.

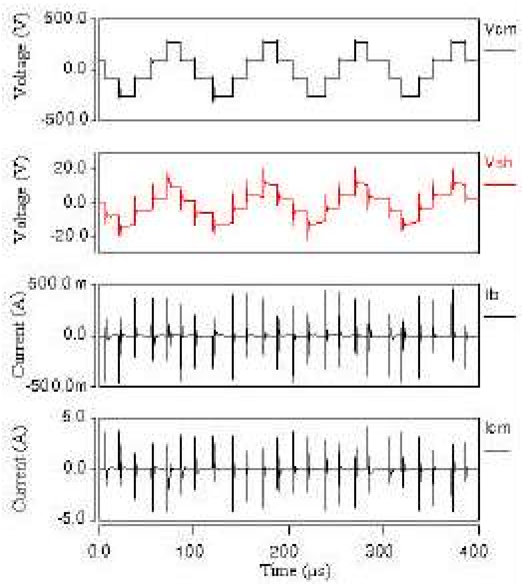

Fig. 10: Predicted common mode voltage, shaft voltage, bearing current and leakage current (Icm) without filter

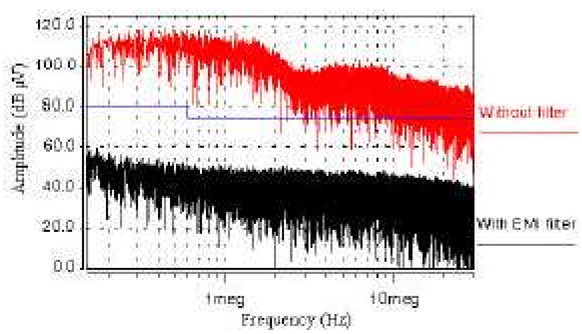

Fig. 11: Comparison between the predicted EMI without and with EMI filter

The simulation results of common mode voltage (V_{CM}), shaft voltage (V_{sh}), bearing current (I_b) and leakage current (I_{CM}) are shown in Fig. 10. the predictions show that shaft voltage between motor shaft and ground appears by 17 volt and bearing current flowing through bearing and ground is about 400mA, leakage current also is 4 A, which can cause of bearing surfaces damage in time due to electric discharge machining (EDM) effect, or electroplating of the race steel and bearing balls. Also predicted EMI couldn't meet the EMI limits (EN55011). But after connecting the proposed filter to system (Fig. 7) EMI reduced. A comparison between the predicted EMI without and with EMI filter is shown in Fig. 11.

Figure 12 shows the predicted shaft voltage, bearing current and leakage current for system with the proposed filter. As shown in Fig. 12 shaft voltage is about several mVs, which cannot cause of any damaging in motor, bearing current and shaft voltage are ignorable.

EXPERIMENTAL RESULTS

Without employing filters the PWM inverter ac motor system constructed to test. The test system included the 3.7 kW induction motor, 6 kVA PWM inverter drive system, line impedance stabilization networks (LISN) and other measuring system for evaluating the adverse effects in the system. Standards regulations call for the utilization of LISN to be placed between ac power supply and the equipment under test (EUT) for measuring EMI. Measured common mode voltage and shaft voltage are shown in Fig. 13. Common mode voltage (V_{CM}) of Fig. 13 is measured from a Y connected node of three capacitors to dc bus midpoint. The measured waveforms of bearing current and common mode current are shown in Fig. 14.

Fig. 15 shows the conducted EMI when no filter connected to the system. After connecting the passive filter to the system almost of the adverse effects are eliminated. The results of common mode voltage and shaft voltage are presented in Fig. 16. The measured bearing current and leakage current is shown in Fig. 17. The effect of filter on conducted EMI reduction is shown in Fig. 18. Figures 16, 17 and 18 show that proposed passive filter could reduce all the adverse effects drastically. Shaft voltage reduced to 100 mV, which cannot be cause of premature motor failures. The bearing current almost is eliminated and also the leakage current is mitigated by employed small passive filter between rectifier input and motor neutral point.

The measured conducted EMI illustrated in Fig. 18 satisfied the EMI regulation of the CISPR 22 class A limit which are limited conducted EMI to below 79 dBμV. CISPR 22 regulation has been used globally for many years to determine compliance of electrical machine drive system with applicable limits as electromagnetic compatibility (EMC) regulation. Many economies like the European Union, Japan, Australia and New Zealand have adopted CISPR 22 into locally applicable standards. Other countries also accepted this regulation as international regulations. In this paper CISPR 22 regulations are considered. Limit of conducted emission of CISPR 22 (last version: 2004) for conducted emissions is 79 dBμV in the range of frequency 0.15-0.5 MHz and 73 dBμV in the range of frequency 0.5-30 MHz that is drawn in conducted EMI spectrum of simulations results (Figure 10). These limits are similar to other standards and regulations such as FCC class A limits (USA standards), EN

55022, IEC 61000 (European standards) and other acceptable standards.

CONCLUSION

The adverse effects of PWM inverter in electrical machine system has concerned in this paper. A passive cancellation method based on two small passive filter connected between motor neutral point and rectifier input and also between inverter output and motor terminal has been proposed, designed and tested for a 6 kW inverter fed 3.7 kW induction motor.

Whole system has been modeled and then simulated by Saber software with and without connecting the proposed passive filter. Experimental results have verified that the proposed passive filter is effective and valuable in preventing the adverse effects of PWM inverter in electrical machine system. The simulation and experimental results had good agreement together.

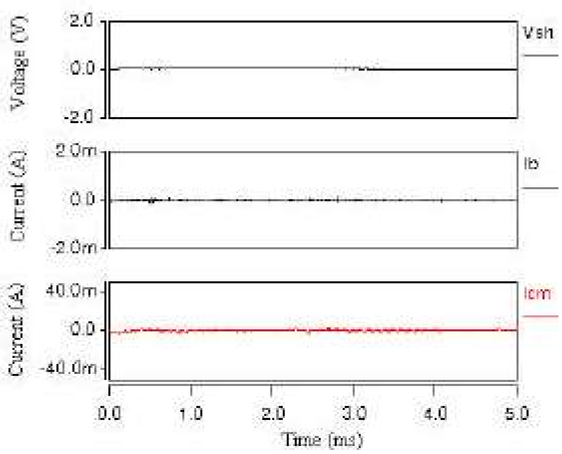

Fig. 12: Shaft voltage, bearing current and leakage current with proposed filter

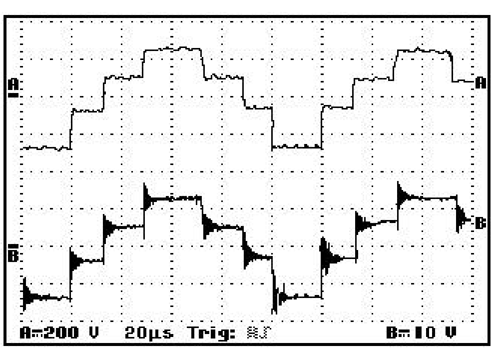

Fig. 13: Measured common mode voltage (A waveform) and shaft voltage (B waveform) without filter

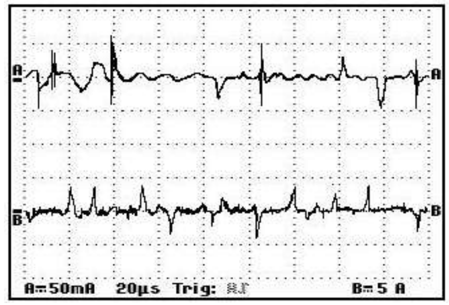

Fig. 14: Measured bearing current (A waveform) and leakage current (B waveform) without filter

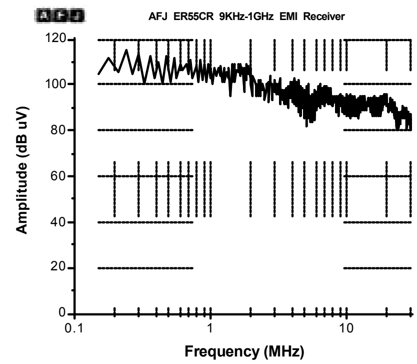

Fig.15: Conducted EMI (without filter)

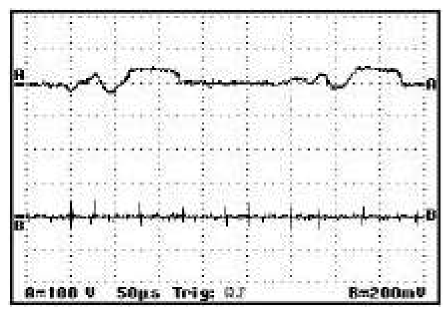

Fig. 16: Measured common mode voltage (A waveform) and shaft voltage (B waveform) (With passive EMI filter)

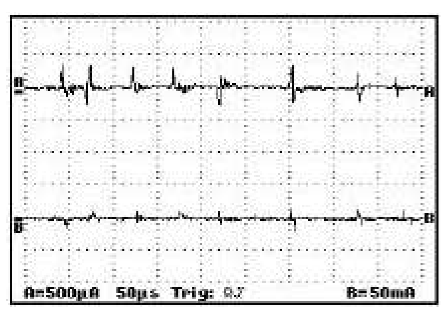

Fig. 17: Measured bearing current (A waveform) and leakage current (B waveform) (With passive EMI filter)

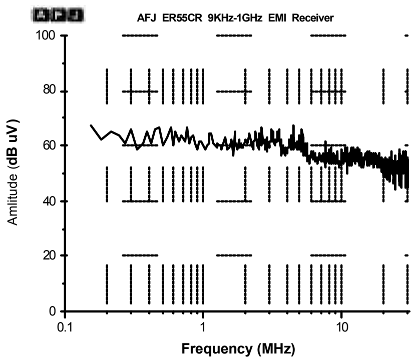

Fig. 18: Conducted EMI (With passive EMI filter)

REFERENCES

1. Vaez-Zadeh, S. and M. Zamanian, 2003. Permanent Magnet DC Motor Sliding Mode Control System. IJE Transaction, A: Basics, 16 (4): 367-376.
2. Zare, Firuz, 2009. EMI Issues in Modern Power Electronic Systems. The IEEE EMC Society Newsletters, 221: 53-58.
3. Akagi, H. and T. Doumoto, 2004. An approach to eliminating high-frequency shaft voltage and ground leakage current from an inverter-driven motor. IEEE Transactions on Industry Applications, 40 (4): 1162-1169.
4. Akagi, H. and T. Doumoto, 2004. A passive EMI filter for preventing high-frequency leakage current from flowing through the inverter heat sink of an adjustable-speed motor drive system. 39th Annual Meeting IEEE Industry Applications Conference, (Oct. 3-7, 2004), 3: 2003-2009.
5. Mei, C., J.C. Balda and W.P. Waite, 2003. Minimization and cancellation of common-mode currents, shaft voltages and bearing currents for induction motor drives. 34th Annual IEEE Power Electronics Specialist Conference, (June 15-19, 2003), 3: 1127-1132.
6. Schiferl, R.F. and M.J. Melfi, 2004. Bearing current remediation options. IEEE Industry Applications Magazine, 10 (4): 40-50.
7. Hyypio, D., 2005. Mitigation of bearing electro-erosion of inverter-fed motors through passive common-mode voltage suppression. IEEE Transactions on Industry Applications, 41 (2): 576-583.
8. Wen, D., L.V. Chuan, J. Jiangguo, 2002. Filter design of restraining over-voltage and bearing current in induction motor fed by PWM inverter. In Proc. of IEEE TENCON'02, pp: 2083-2086.
9. Chen, X., D. Xu, F. Liu and J. Zhang, 2007. A Novel Inverter-output passive filter for reducing both different and common dv/dt at the motor terminals in PWM drive system. IEEE Transaction on Industrial electronics, 54: 419-426.
10. Weiming, M., Z. Zhihua, M. Jin, P. Qijun and Z. Lei, 2008. Precise methods for conducted EMI modeling, analysis and prediction. Science in China, 51 (6): 641-655.
11. Salomäki, J., M. Hinkkanen and J. Luomi, 2006. Influence of Inverter Output Filter on the Selection of PWM Technique. IEEE ISIE 2006, Montréal, Québec, Canada, (July 9-13, 2006), pp: 1052-1057.
12. Lu, Y., Z. Chen and H. Huang, 2007. The System for the Reduction of Conducted Electromagnetic Interference Emission from Switching Power Supply. Third International Conference on Intelligent Information Hiding and Multimedia Signal Processing, Splendor Kaohsiung, Taiwan, (Nov. 26-28, 2007), 2: 397-402.
13. Poire, Y., O. Maurice, M. Ramdani, H. Drissi and A. Sauvage, 2007. SMPS Tools for EMI Filter Optimization. 18th International Zurich Symposium on Electromagnetic Compatibility, Munich, Germany, (Sep. 24-28, 2007), pp: 505- 508.
14. Drinovsky, J., J. Svacina and Z. Raida, 2008. Potential Worst-case System for Testing EMI Filters Tested on Simple Filter Models. Radio Engineering, 17 (3): 15-18.
15. SABER, Analogy, Inc., 9205 S.W. Gemini Drive, Beaverton, OR 97008, USA, Release 5.1 Edition.
16. Esmaeli, A. and L. Sun, 2007. Modeling and simulation of induction motor drive system to investigate and mitigate of PWM inverter's adverse effects. Journal of Harbin Institute of Technology, 14 (1): 83-88.
17. Mirafzal, B., G. Skibinski and R. Tallam, 2009. Determination of parameters in the universal induction motor model. IEEE Transactions on Industry Applications, 45: 142-151.
18. Agilent 4285A, Precision LCR Meter Data Sheet.